Physicochem. Probl. Miner. Process., 55(5), 2019, 1059-1069

http://www.journalssystem.com/ppmp

Physicochemical Problems of Mineral Processing

ISSN 1643-1049

Received February 02, 2019; reviewed; accepted April 26, 2019

QSAR study of amine collectors for iron ore reverse flotation

Benying Wang, Xinyang Xu, Hao Duan, Xinyang Wang

School of Resources and Civil Engineering, Northeastern University, Shenyang 110819, China

Corresponding author: Xuxinyang@mail.neu.edu.cn (Xinyang, Xu); duanhao.once@gmail.com (Hao, Duan)

Abstract: In order to reveal the relationship between flotation behaviors of collectors and their structures, quantitative structure–activity relationship (QSAR) study about separation efficiency of quartz from hematite using amine collectors was performed. The genetic function approximation (GFA) algorithm was applied to generate the correlation models and model with acceptable R^2 and R_{cv}^2 (cross validated R-squared) correlation coefficients (R^2=0.9666, R_{cv}^2=0.9201) was developed. The model revealed that the Lowest Unoccupied Molecular Orbital (LUMO) energy of the molecule, the charge of nitrogen and the electronegativity of polar group were the major factors that affected the separation efficiency of collectors. The higher nitrogen charge, the larger electronegativity of polar group and the more positive of LUMO energy of amine collectors were, the higher separation efficiency would be.

Keywords: QSAR, separation efficiency, reverse flotation, amine collectors

1. Introduction

Quartz is the common mineral associated with almost all kinds of minerals, especially in iron ores (Araujo et al., 2005; Sahoo et al., 2015). Except quartz is collected as useful mineral, quartz has to be removed from valuable minerals to reduce its negative impact on the following up industrial procedure such as blast furnace smelting (Laitinen et al., 2016; Li et al., 2017; Liu et al., 2019). Reverse cationic flotation of quartz provided an effective way to remove quartz from iron ores, and with the development of cationic collectors, the shortages of primary fatty amines such as poor selectivity, low flotation speed and excessive foam has been improved (Yu et al., 2008; Filippov et al., 2014).

As we know, chemical reactivity and physicochemical properties of compounds are determined by their molecular structures. In the development of flotation reagents, most of researches focused on the synthesis novel collectors and their application in flotation process (Huang et al., 2014; Brezani et al., 2017; Liu et al., 2017), and the relationship between collectors' molecular structures and flotation behaviors still remains uncertain. Ackerman (Ackerman et al., 2000) investigated the influence of different substituents of xanthogen formats in the flotation of copper sulfide minerals, and the results demonstrated that the flotation behavior of copper sulfide minerals was closely related to chain length, branch degrees of substituents and type of substituents. Natarajan et al. (Natarajan and Nirdosh, 2009) studied the substituents effect of the N-arylhydroxamic acids in the flotation of copper-nickel ore and the results showed that the position of substituents have a significant impact on the flotation behaviors. Liu et al. (Liu et al., 2009) conducted flotation tests for kaolinite using a series of tertiary amines and the results indicated that the inductive electronic effects and space steric effects of substituent group bound to the N atom result in different collecting powers for tertiary amines. In this work, the relationship between molecular structures of collectors and their flotation behavior differences were presented in the qualitative level without further statistical processing and analysis. However, determining the quantitative relationship is very important for the development of flotation reagents.

QSAR, a modeling method which correlates the activity of a series of compounds with their structure descriptions (Karelson et al., 1996), has been widely applied in chemical, biological, and pharmaceutical activities (Kar and Roy, 2010; Shahlaei, 2013). In mineral processing filed, QSAR has also been utilized

DOI: 10.5277/ppmp19028

to investigate the relationship between flotation performance and molecular structure of collectors. But most work conducted the QSAR research for sulfide mineral collectors (Natarajan and Nirdosh, 2003, 2006, 2008, 2009; Yang et al., 2012; Yang et al., 2018a). The QSAR study for oxide minerals collectors was relatively less (Natarajan et al., 2002; Yang et al., 2018b), especially for the amine collectors in oxide minerals flotation, Hu et al. (Hu et al., 2012) used 20 quaternary ammonium salts to explore the relationship between the collectors' structure and their selectivity in bauxite reverse flotation and established a robust model. And in Hu's study, all of the amine collectors they chosen were quaternary ammonium salts. Thus, in order to provide basic data for research in this field and enrich database of amine collectors, this work conducted the QSAR research of amine collectors (including primary amine, secondary amine, tertiary amine, quaternary ammonium salts and hydroxyl-alkyl amine) for oxide minerals. Besides, this work focused on the influence of polar groups (non-polar group was dodecyl to ensure the hydrophobicity (Somasundaran et al., 1964; Novich and Ring, 1985; de Medeiros and Baltar, 2018)) in the flotation separation of quartz and hematite, which provided an insight into the design high efficient polar group of amine collectors for hematite reverse flotation.

2. Materials and methods

2.1. Materials and reagents

Samples of quartz and hematite were obtained from Qidashan Iron Mine, Liaoning province of China. The samples were carefully hand-picked, crushed, and ground in a laboratory porcelain mill. Then the samples were wet-sieved to obtain the -0.074 mm fraction, then the samples were further purified by shaking table. Besides, the quartz particles were leached with hydrochloric acid for three times, once every 24 h. Chemical compositions of hematite and quartz samples were listed in Table 1, and the purities of hematite and quartz were 98.14% and 99.18%, respectively. The X-ray diffraction pattern results (Fig. 1) confirmed that the main minerals in pure samples are hematite and quartz. Therefore, the samples were sufficiently pure to meet the requirement for experiments.

Table 1. Chemical compositions of pure minerals (wt%)

Sample	Fe_2O_3	SiO_2	Al_2O_3	MgO	CaO	P	S
Hematite	98.14	1.01	0.21	0.1	0.02	0.01	0.35
Quartz	0.02	99.18	0.45	0.05	0.04	0.01	0.14

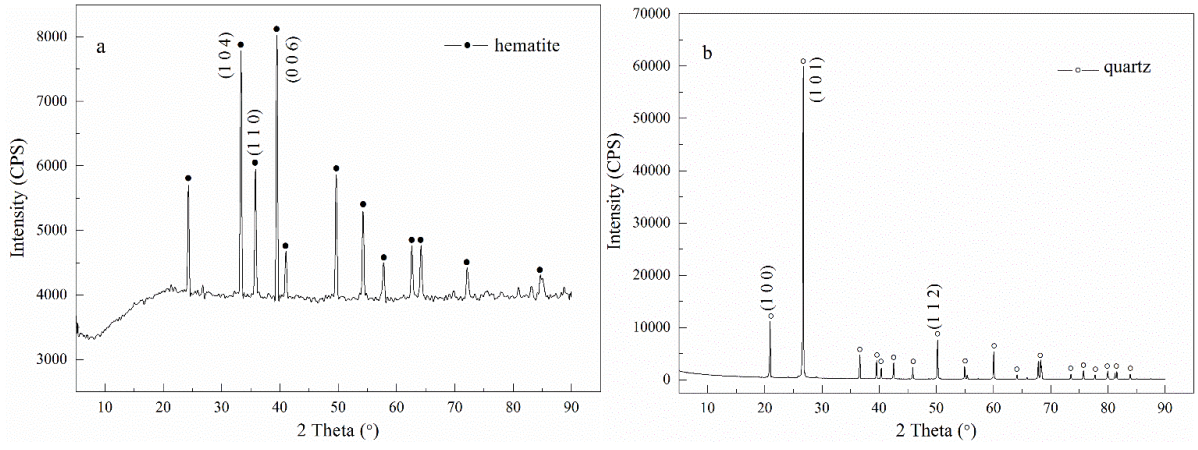

Fig. 1. X-ray diffraction spectra of hematite (a) and quartz (b)

The detailed information about collectors used in this experiment were given in Table 2. 1-(Dodecylamino)-2-propanol (DAP), N,N-Bis (2-hydroxypropyl) dodecylamine (NNHPA) and Bis (2-hydroxy-3-chloropropyl) dodecylamine (HCA) were synthesized in laboratory (Liu et al., 2016; Liu et al., 2017; Liu et al., 2018). Besides, the other seven collectors as Dodecylamine (DDA), N-Methyl-N-dodecylamine (NMDA), N,N-Dimethyl -N-dodecylamine (NNDDA), Dodecyltrimethylammonium chloride (DTAC), Dodecyl trimethyl ammonium bromide (DTAB), Dodecyl ethyl dimethyl ammonium

bromide (DEDAB), N,N-Bis (2-hydroxyethyl) dodecylamine (NNHEA) with more than 97% analytical purities were purchased from J&K Scientific Co. Ltd. HCl and NaOH solutions with a concentration of 0.1 mol/L were used as pH regulator. Deionized water was used in all experiments.

2.2. Micro-flotation

Single mineral flotation tests were conducted in a 40 mL XFG II flotation cell (Jilin Prospecting Machinery Factory, China). In Single mineral flotation test, 2.0 g mineral samples were placed in the cell with 30 mL deionized water. After that, the pulp was stirred for 2 min with the agitator speed of 1800 rpm. Then, pH regulator and collector were added into the pulp in sequence. Conditioning time of each reagent was 2 min, and the flotation time was 5 min. For the artificially mixed mineral separation tests, 2 g samples (1.2 g hematite and 0.8 g quartz) was mixed with 30 mL deionized water in the flotation cell. The subsequent steps were the same as in the single mineral flotation test. Both concentrates and tailings were filtered, dried, weighted and assayed to calculate the yield, recovery and grade.

2.3. Structure parameter calculation

The Quantum parameter calculations were performed by DMol3 module in Materials Studio 6.0 (2012). The computation was based on Perdew-Burke-Ernzerhof correlation (PBE) of non-local gradient-corrected exchange-correlation functionals (GGA). All Electron Relativistic was chosen for the core treatment and the basic set was Double Numerical plus d-functions (DND). For self-consistent electronic minimization, the Pulay density mixing method was used with a SCF convergence tolerance of 1.0×10^{-6}. And convergence criteria fixed for the energy, maximum force and maximum displacement tolerance were 1.0×10^{-5} Ha, 0.002 Ha/Å and 0.005 Å, respectively (Hammer et al., 1999). Topological indices were 2D descriptors based on graph theory concepts, and they were calculated by the theoretical formulas which programmed in QSAR module of Materials Studio. Parts of physicochemical parameters of collectors were calculated by the QSAR module in Materials Studio, and the others were calculated by theoretical formulas.

2.4. QSAR model building

In this study, the Genetic Function Approximation (GFA) algorithm was applied to build the QSAR models for its overfitting resistance, accuracy and celerity compared with other methods (Rogers and Hopfinger, 1994; Shi et al., 1998; Sivakumar et al., 2007; Khaled, 2011). The population and maximum generations were 200 and 5000, respectively. Friedman lack-of-fit measure (Friedman LOF) was used to evaluate the quality of model, and the smoothness parameter was 0.5.

3. Results and discussion

3.1 Separation efficiency calculation

Flotation is a separation process, and recovery (ε), grade (β) and yield (γ) were frequently used to assessment the flotation behaviors, but it's incomplete to judge flotation process using one single parameter. Thus, we chose separation efficiency (SE), a comprehensive parameter to evaluate separation behaviors, as the dependent variable in QSAR models building. And it was calculated by Eq. (1) (Hancock, 1920).

$$\mathrm{SE} = \frac{\varepsilon-\gamma}{\beta_{max}-\alpha}\beta_{max} \tag{1}$$

where ε is the recovery of concentrate, γ is the yield of concentrate, α is the iron grade of the artificial ore, and β_{max} (70%) is maximum grade of concentrate.

According to the single mineral flotation results, as shown in Fig. 2 and 3, ten amine collectors both exhibited good floatability for quartz with the increasing dosage of collectors, while the recovery for hematite varied from different collectors. When the dosage increased to 16 mg/L, the recovery of quartz showed little variation. And at neutral environment, quartz could be easily floated by ten amine collectors. Base on the single mineral flotation results, the artificially mixed minerals separation

experiments were conducted with collector concentration of 16 mg/L at natural slurry pH and the separation results and corresponded SE values are shown in Table 2.

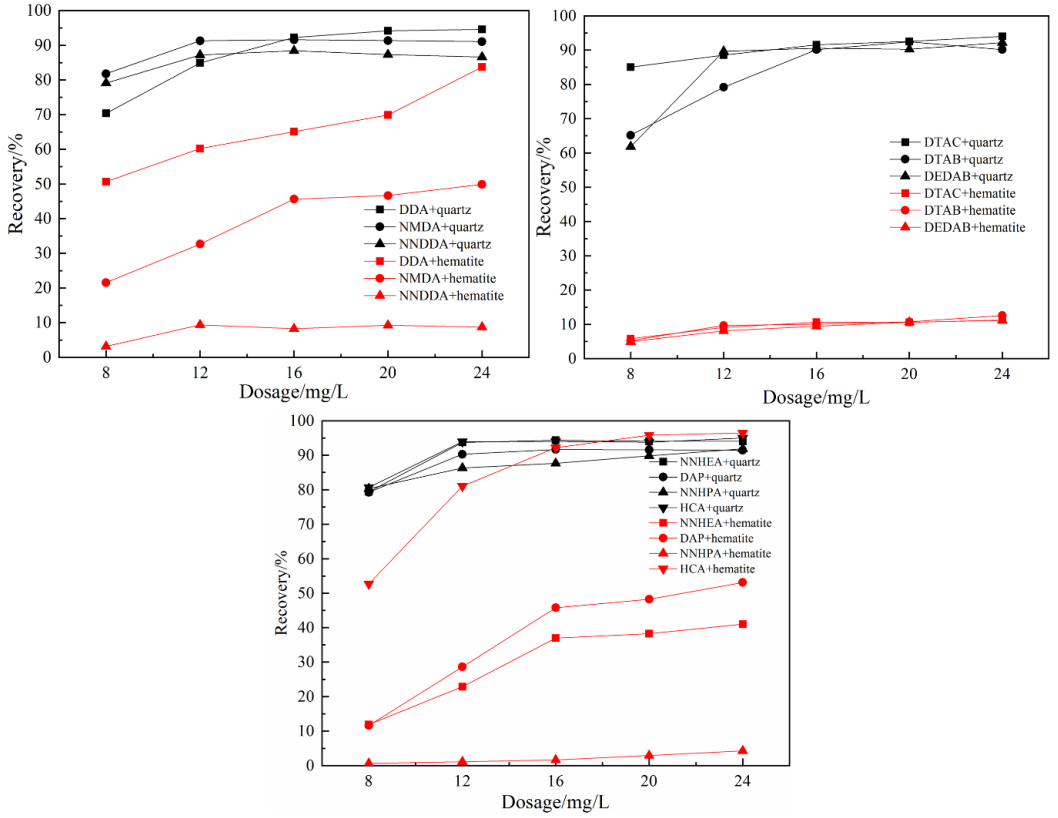

Fig. 2. Recovery of quartz and hematite as a function of dosage

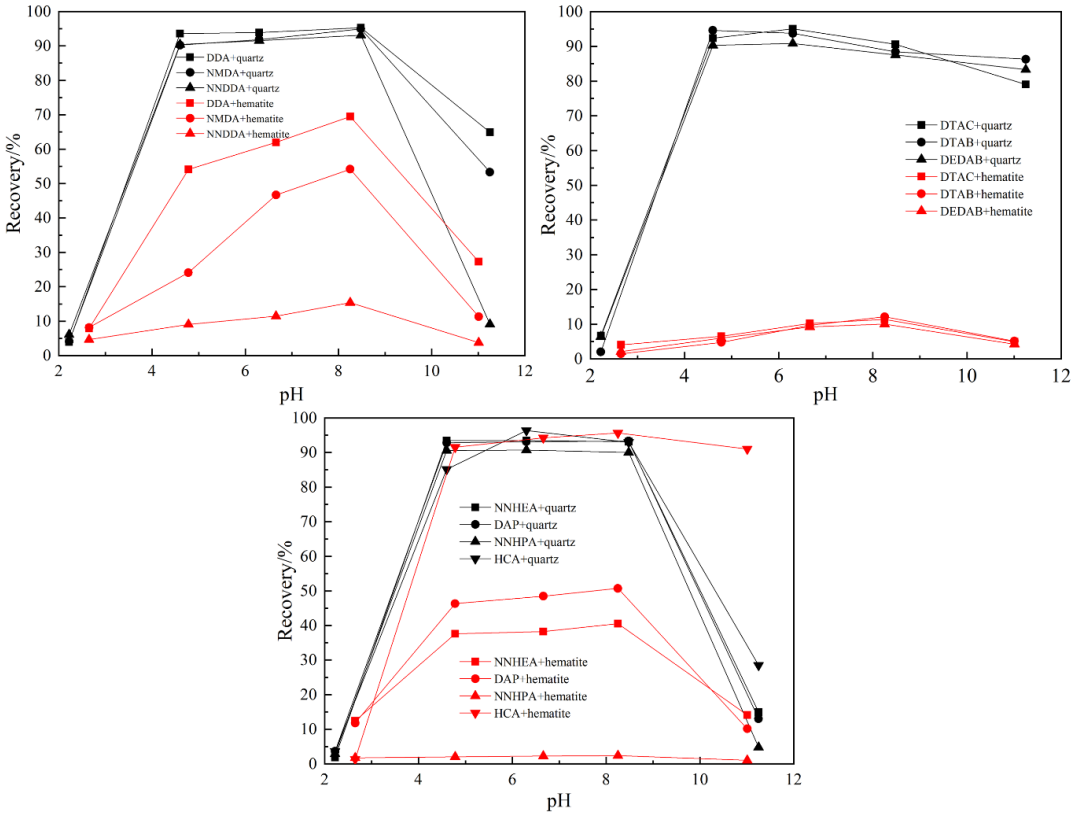

Fig. 3. Recovery of quartz and hematite as a function of pH

Table 2. Separation results of artificially mixed minerals and SE values

Collectors	abbreviation	α/%	β/%	γ/%	ε/%	SE/%
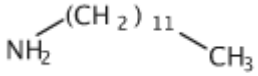	DDA	41.25	62.09	33.91	51.04	41.71
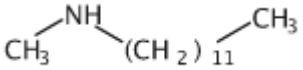	NMDA	41.27	66.85	40.30	65.28	60.86
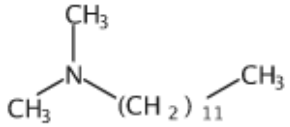	NNDDA	41.26	66.20	52.75	84.64	77.67
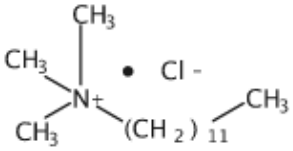	DTAC	41.25	65.42	53.78	85.29	76.72
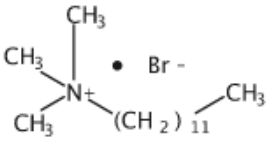	DTAB	41.23	64.33	57.06	89.03	77.79
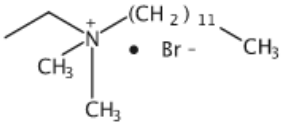	DEDAB	41.23	64.30	57.57	89.78	78.37
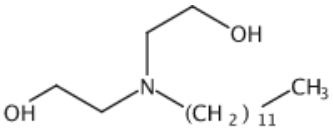	NNHEA	41.34	65.92	53.68	85.60	77.96
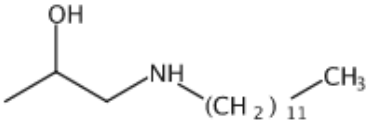	DAP	41.45	64.40	39.93	62.04	54.21
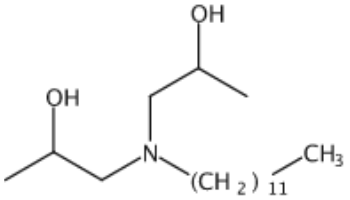	NNHPA	41.29	64.65	57.49	90.02	79.31
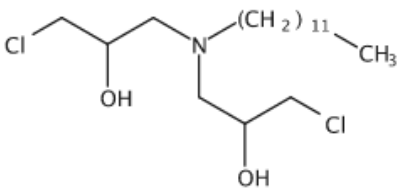	HCA	41.25	60.58	29.19	42.87	33.31

Although the above collectors have same non-polar group, dodecyl, the separation results were different due to the different configuration of polar group. When the hydrogen of amine group (DDA) substituted by methyl (structures like NMDA and NNDDA), the SE value increased with the branching degrees increased. In the case of DAP and NNHPA, when the substitute group, isopropyl, increased from one (DAP) to two (NNHPA), the SE value raised from 54.21% to 79.31%, which also indicated that the SE was closely related to branch degrees. When NNHEA, DAP, NNHPA and HCA used as collector, the SE value was significant changed, which indicated that the introduced functional group have a

prominent influence on the separation results. In summary, both of the branching degrees of polar group and the functional group have significant effect on separation efficiency. To determine the quantitative relationship between collectors' molecular structure and their separation efficiency, the structure parameters of collectors were calculated for develop of QSAR model.

3.2. Structure parameter calculation

Choosing the appropriate parameters in QSAR model building determined whether the QSAR models could support the follow-up researches. Thus, it is essential to select proper structure parameters in QSAR model building process (Mansouri et al., 2013; Shahlaei, 2013).

The flotation results revealed that the separation efficiency was closely related to the structure of molecule. Molecular connectivity index ($^n\chi$), valence connectivity index ($^n\delta^v$), shape index (^nK) and its amendment ($^nK^v$) can characterize the molecular structure very well in numerical form (Randic, 1975; Devillers and Balaban, 2000; Todeschini and Consonni, 2008). And they had been widely utilized in QSAR research of flotation (Natarajan et al., 2002; Hu et al., 2012), thus, these topological indices were chosen for QSAR model building in our work. The calculation results are shown in Table 3.

Quantum parameters revealed the inner molecular structure in a more accurate form (Karelson et al., 1996). HOMO (highest occupied molecular orbital) and LUMO (lowest unoccupied molecular orbital) energy are associate with chemical reactivity and band gap (HOMO-LUMO) is an important stability index, and both of them have been widely used to explain flotation behaviors (Ahamad et al., 2010; Liu et al., 2013). The charge of nitrogen revealed the strength of electrostatic adsorption between collectors and minerals (Liu et al., 2015). Dipole moment (μ) and molecular force field parameters (energy parameters) were also frequently used to explain flotation results and had been widely applied in QSAR researches (Eroglu and Türkmen, 2007; Diao et al., 2010). Thus, these quantum parameters were chosen as structure descriptions and the corresponding calculation results are shown in Table 4.

The formation of hydrogen bond has a significant influence on the adsorption between amine collectors and minerals (Gao et al., 2015). Thus, HBA (Hydrogen Bond Acceptor) and HBD (Hydrogen Bond Donor) were chosen as physicochemical parameters in QSAR model and they were calculated in QSAR module. HLB (Hydrophilic lipophilic balance) and log P (Octanol-Water Partition Coefficient) provided an insight into the hydrophobic of collectors (Vaziri Hassas et al., 2014; Deng et al., 2016; Wang et al., 2018). log P was calculated in QSAR module, and HLB was calculated by Eq. (2) (Liu et al., 2018). Electronegativity of group (x_g) was closely related to the flotation efficiency and it was calculated by Eq. (3) and (4) (Wilmshurst, 1957). Other geometrical parameters, such as surface area, molecular density, and molecular volume et al. could characterize the molecular structure in macroscopic level. These properties affected the flotation behavior and had been widely used in QSAR model building (Basak et al., 1997) and they were calculated in QSAR module. The calculation results are shown in Table 5.

$$\mathrm{HLB} = \frac{\sum(hydrophilic\ group\ index)}{\sum(hydrophobic\ group\ index)} \times 10 \tag{2}$$

$$x_g = 0.31\frac{n^*+1}{r} + 0.5 \tag{3}$$

$$n^* = (n-p) + 2m\frac{x_A}{x_A+x_B} + s\frac{x_A}{x_A+x_B} \tag{4}$$

where hydrophilic/hydrophobic group index were obtained from Wang's research (Wang et al., 1996; Liu et al., 2018), x_g was electronegativity of group, n^* was the actual valence electrons of A in the AB bond, r was the covalent radius of A atom, n was the valence electrons of A atom, p was the electron number bonded by B atom, m was the number of bonding electrons between A and B atom, s was the number of resonance, x_A and x_B was the pauling electronegativity of A and B, respectively (Wilmshurst, 1959; Wang et al., 1996).

3.3. Model building and validation

GFA algorithm was employed to complete statistical analysis, nine of collectors were used as training set to build models and DTAB was used to test the predictive ability of the models. The best model built by GFA method was listed below.

$$SE=30.3381X1+145.2632X2+22.6595X3-58.3151 \tag{M1}$$

Table 3. The topological indices used in the construction of QSAR models

collectors	DDA	NMDA	NNDDA	DTAC	DTAB	DEDAB	NNHEA	DAP	NNHPA	HCA
^{1}K	13.00	14.00	15.00	16.00	16.00	17.00	19.00	17.00	21.00	23.00
^{2}K	12.00	13.00	12.07	10.17	10.17	11.11	16.06	14.06	14.92	16.84
^{3}K	12.00	13.09	14.00	15.07	15.07	12.25	14.22	16.00	16.20	15.28
$^{1}K^{v}$	12.96	13.96	14.96	15.96	15.96	16.96	18.88	16.92	20.88	23.46
$^{2}K^{v}$	12.00	13.00	12.03	10.14	10.14	11.07	15.94	13.98	14.80	17.29
$^{3}K^{v}$	12.00	13.05	14.00	15.04	15.04	12.21	14.10	15.92	16.08	15.71
$^{0}\chi$	9.78	10.48	11.36	12.28	12.28	12.99	14.18	12.77	15.92	17.34
$^{1}\chi$	6.41	6.91	7.27	7.56	7.56	8.12	9.35	8.27	10.06	11.13
$^{2}\chi$	4.18	4.54	5.36	6.49	6.49	6.45	6.41	6.07	8.10	8.33
$^{0}\delta^{v}$	9.36	10.28	11.23	12.23	12.23	12.93	12.95	12.01	14.69	16.37
$^{1}\delta^{v}$	6.12	6.56	6.92	7.36	7.36	7.94	8.29	7.66	9.14	10.41
$^{2}\delta^{v}$	3.97	4.29	4.99	6.20	6.20	6.16	5.47	5.24	6.64	7.18

Table 4. The quantum parameters used in the construction of QSAR models

collectors	DDA	NMDA	NNDDA	DTAC	DTAB	DEDAB	NNHEA	DAP	NNHPA	HCA
HOMO	-5.20	-4.87	-4.72	-3.93	-3.79	-3.71	-4.63	-5.41	-4.85	-5.41
LUMO	1.30	1.38	1.41	-0.02	-0.02	-0.02	0.84	1.02	0.59	-0.85
Band gap	6.50	6.25	6.13	3.92	3.57	3.69	5.47	6.43	5.44	4.56
Binding	-6.00	-6.45	-6.90	-7.51	-7.48	-7.95	-8.15	-7.55	-9.08	-9.01
electrostatic	17.43	18.06	-6.42	-35.92	-30.47	-16.91	29.15	-	-35.06	41.08
van der	2.16	3.61	7.25	32.68	23.96	25.16	10.47	12.13	14.77	20.97
Non band	19.59	21.67	0.83	-3.25	-6.52	8.25	39.62	-0.50	-20.30	62.97
Bond energy	3.74	3.47	3.68	14.76	14.78	17.46	17.28	11.15	23.47	23.04
Torsion	0.12	0.18	0.29	0.24	0.18	0.21	1.36	0.35	1.94	2.37
Angle	10.44	10.28	12.17	13.81	13.26	17.46	17.28	11.15	23.47	23.04
Valence	14.30	13.93	16.14	28.81	28.22	34.97	26.03	16.74	34.80	34.66
Total energy	-529	-568	-608	-1109	-3216	-3255	-837	-722	-916	-
μ	0.57	0.37	0.21	5.09	5.42	5.36	0.46	1.16	1.42	1.27
μ_x	-0.17	0.34	0.18	0.58	0.61	0.75	-0.09	0.45	1.31	1.11
μ_y	0.34	-0.08	-0.11	-0.86	-0.94	-0.40	-0.11	-0.66	0.49	0.39
μ_z	-0.43	-0.13	-0.03	-4.98	-5.30	-5.29	0.44	-0.84	0.26	-0.49
Atom charge (N)	-0.23	-0.16	-0.10	0.11	0.11	0.10	-0.08	-0.14	-0.08	-0.07

Table 5. The physicochemical parameters used in the construction of QSAR models

collectors	DDA	NMDA	NNDDA	DTAC	DTAB	DEDAB	NNHEA	DAP	NNHPA	HCA
HLB	2.92	2.69	2.50	13.12	12.35	11.34	8.44	5.67	7.50	7.38
χ_g	3.99	4.48	4.63	5.26	5.26	5.44	5.50	4.79	5.64	5.66
log P1	4.41	4.49	5.13	3.28	3.28	3.82	2.48	3.32	3.17	4.33
log P2	3.77	4.17	4.53	4.06	4.06	4.40	3.65	4.13	4.47	5.20
HBD	2.00	1.00	0.00	0.00	0.00	0.00	2.00	2.00	2.00	2.00
HBA	1.00	1.00	1.00	0.00	0.00	0.00	3.00	2.00	3.00	5.00
Molecular	226.6	243.4	261.4	300.8	306.3	322.9	311.2	285.3	345.8	374.0
Molecular	0.82	0.82	0.82	0.88	1.01	1.00	0.88	0.85	0.87	0.99
Surface area	309.2	325.8	349.8	400.0	404.2	421.9	415.0	382.8	459.0	492.1
Connoly	277.1	296.7	312.1	346.8	351.9	365.8	365.1	343.1	393.9	422.9
Connoly surface occupied	245.9	260.7	278.5	319.1	327.3	343.8	333.3	303.0	370.3	403.1

Note: log P1 and log P2 was calculated using two different methods.

R^2=0.9666 R^2_{ad}=0.9461 R^2_{CV}=0.9201 F=81.8731

where X1 is LUMO energy of the collector, X2 is the charge of nitrogen, X3 is the electronegativity of group.

R-squared (R^2), Adjusted R-squared (R_{ad}^2), Cross validated R-squared (R_{cv}^2) and F-value were frequently used to measurement the fitness and prediction ability of the model in statistics study (Sabljic, 2001; Hu et al., 2012). In general, the closer of R^2 value to 1, the better fitness of the model would be. The similarity between R^2 and R_{ad}^2 indicates that the number of independent variables is suitable. F means the significance level of the model. R_{cv}^2 shows the predict ability of the model. The model is identified to have good predict ability when the R_{cv}^2 value of the model more than 0.6. In our study, R^2=0.9666 and R_{cv}^2=0.9201 indicated that M1 was well fitted and had good predict ability. The F value of model was far bigger than threshold value (5.636), which meant the significance of M1 was very well.

To further validate the fitness and predict ability of M1, the correlation between experimental SE value and calculated SE based on M1 is shown in Fig. 4.

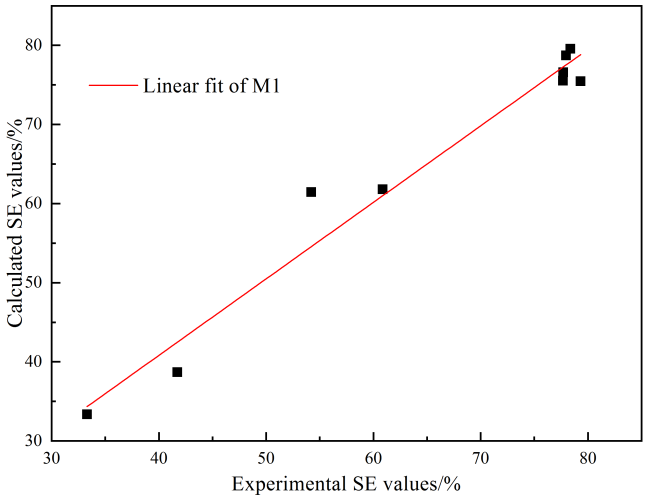

Fig. 4 Fitted curve between experimental and calculated SE values (Y=0.96662X+2.5151, Error=0.0679, SD=4.5301, R=0.9619)

where Y and X are denoted as calculated and experimental SE values, respectively. Error referred to the difference between the average value of y and that of x multiplied with the regression coefficient, R was the linear relativity index, SD was the standard deviation used to measure the dispersion degree of a set of data values. In statistics, the closer to zero of the error and SD, the better the fitness of the curve would be. The fitted curve in Fig. 4 indicated that the M1 was well fitted and had the good predict ability, which in consistence with the statistics analysis of M1.

A credible and reliable QSAR model requires not only the high fitting of internal data but also the accurate prediction of external data. However, in the mineral processing field, there was not enough data to establish such a database. For this reason, on the premise of the essential data to establish the QSAR model, DTAB was extracted for the external test of the M1. The predicted SE value for DTAB was 76.20% and the experimental value was 77.79%, which indicated that the predicted SE and the experimental SE were in good consistence.

3.4. Interpretation of QSAR model

M1 demonstrated that the LUMO energy of the molecule, the charge of nitrogen and the electronegativity of polar group were positive correlated with SE. It seems a bit of surprising that LUMO energy is related to SE because HOMO energy is usually used to evaluate the flotation behaviors (Deng et al., 2017). In general, high HOMO energy means the molecule is easily to lose its electrons, while high LUMO energy means that the molecule is hard to gain electrons. The adsorption of amine collectors to minerals surface is mainly through electrostatic force and hydrogen bond force (Li et al., 2017; Liu et al., 2017). That is, the higher LUMO energy means that the collectors are more likely to be positive charged and adsorb on the negative charged quartz surface. The strength of electrostatic attraction force is directly influenced by the charge of nitrogen in the molecule (Zhu et al., 2016; Zhang et al., 2017). The high charge of nitrogen may induce the electrostatic repulsion between the collectors and hematite, thus improve the selectivity of collectors. The total free energy change (ΔE) in the flotation process can be expressed by Eq. (5). $\Delta E_{non\text{-}polar}$ can be expressed by Eq. (6). When the physical adsorption is dominated in the flotation process, ΔE_{polar} can be defined as Eq. (7) (Wang et al., 1996). In this study, the non-polar of all collectors were dodecyl. Therefore, $\Delta E_{non\text{-}polar}$ of the collectors are equal and ΔE has a positive correlation with the electronegativity of group. Thus, the high value of the electronegativity of group benefits the flotation process.

$$\Delta E=\Delta E_{non\text{-}polar}+\Delta E_{polar} \quad (5)$$

$$\Delta E_{non\text{-}polar}=n\omega \quad (6)$$

$$\Delta E_{polar}=a(x_g-x_m)^2+b \quad (7)$$

where $\Delta E_{non\text{-}polar}$ is the free energy change of non-polar group and ΔE_{polar} is the free energy change of polar group, n is the number of methylene in the straight alkyl chain and ω is the energy of methylene, x_g is the electronegativity of group, x_m is the electronegativity of the atom in the flotation minerals, both a and b are the constants.

4. Conclusions

The QSAR research about the separation efficiency of amine collectors and their molecular structures in flotation separation of quartz from hematite was performed with GFA algorithm. According to the statistical analysis and external validation, the model was confirmed to be convincible and reliable. LUMO energy of the molecule, the charge of nitrogen, and the electronegativity of polar group were positive correlated with the separation efficiency based on the analysis of the model.

Reference

ACKERMAN, P.K., HARRIS, G.H., KLIMPEL, R.R., APLAN, F.F., 2000. *Use of xanthogen formates as collectors in the flotation of copper sulfides and pyrite*. Int. J. Miner. Process. 58, 1-13.

AHAMAD, I., PRASAD, R., QURAISHI, M.A., 2010. *Thermodynamic, electrochemical and quantum chemical investigation of some Schiff bases as corrosion inhibitors for mild steel in hydrochloric acid solutions*. Corros. Sci. 52, 933-942.

ARAUJO, A.C., VIANA, P.R.M., PERES, A.E.C., 2005. *Reagents in iron ores flotation*. Miner. Eng. 18, 219-224.

BASAK, S.C., GUTE, B.D., GRUNWALD, G.D., 1997. *Use of topostructural, topochemical, and geometric parameters in the prediction of vapor pressure: A hierarchical QSAR approach*. J. Chem. Inf. Comp. Sci. 37, 651-655.

BREZANI, I., SKVARLA, J., SISOL, M., 2017. *Reverse froth flotation of magnesite ore by using (12-4-12) cationic gemini surfactant*. Miner. Eng. 110, 65-68.

DE MEDEIROS, A.R.S., BALTAR, C.A.M., 2018. *Importance of collector chain length in flotation of fine particles*. Miner. Eng. 122, 179-184.

DENG, L., ZHAO, G., ZHONG, H., WANG, S., LIU, G., 2016. *Investigation on the selectivity of N-((hydroxyamino)-alkyl) alkylamide surfactants for scheelite/calcite flotation separation*. J. Ind. Eng. Chem. 33, 131-141.

DEVILLERS, J., BALABAN, A.T., 2000. *Topological indices and related descriptors in QSAR and QSPAR*. CRC Press.

DIAO, J., LI, Y., SHI, S., SUN, Y., SUN, Y., 2010. *QSAR models for predicting toxicity of polychlorinated dibenzo-p-dioxins and dibenzofurans using quantum chemical descriptors*. B. Environ. Contam. Tox. 85, 109-115.

EROGLU, E., T RKMEN, H., 2007. *A DFT-based quantum theoretic QSAR study of aromatic and heterocyclic sulfonamides as carbonic anhydrase inhibitors against isozyme, CA-II*. J. Mol. Graph. Model. 26, 701-708.

FILIPPOV, L.O., SEVEROV, V.V., FILIPPOVA, I.V., 2014. *An overview of the beneficiation of iron ores via reverse cationic flotation*. Int. J. Miner. Process. 127, 62-69.

GAO, Z., SUN, W., HU, Y., 2015. *New insights into the dodecylamine adsorption on scheelite and calcite: An adsorption model*. Miner. Eng. 79, 54-61.

HAMMER, B., HANSEN, L.B., N RSKOV, J.K., 1999. *Improved adsorption energetics within density-functional theory using revised Perdew-Burke-Ernzerhof functionals*. Phys. Rev. B. 59, 7413-7421.

HANCOCK, R., 1920. *Efficiency of classification*. Eng. Min. J. 110, 622-628.

HU, Y.H., CHEN, P., SUN, W., 2012. *Study on quantitative structure-activity relationship of quaternary ammonium salt collectors for bauxite reverse flotation*. Miner. Eng. 26, 24-33.

HUANG, Z.G., ZHONG, H., WANG, S., XIA, L.Y., ZOU, W.B., LIU, G.Y., 2014. *Investigations on reverse cationic flotation of iron ore by using a Gemini surfactant: Ethane-1,2-bis(dimethyl-dodecyl-ammonium bromide)*. Chem. Eng. J. 257, 218-228.

KAR, S., ROY, K., 2010. *QSAR modeling of toxicity of diverse organic chemicals to Daphnia magna using 2D and 3D descriptors*. J. Hazard. Mater. 177, 344-351.

KARELSON, M., LOBANOV, V.S., KATRITZKY, A.R., 1996. *Quantum-chemical descriptors in QSAR/QSPR studies*. Chem. Rev. 96, 1027-1043.

KHALED, K.F., 2011. *Modeling corrosion inhibition of iron in acid medium by genetic function approximation method: A QSAR model*. Corros. Sci. 53, 3457-3465.

LAITINEN, O., HARTMANN, R., SIRVIO, J.A., LIIMATAINEN, H., RUDOLPH, M., AMMALA, A., ILLIKAINEN, M., 2016. *Alkyl aminated nanocelluloses in selective flotation of aluminium oxide and quartz*. Chem. Eng. Sci. 144, 260-266.

LI, X.B., ZHANG, Q., HOU, B., YE, J.J., MAO, S., LI, X.H., 2017. *Flotation separation of quartz from collophane using an amine collector and its adsorption mechanisms*. Powder. Technol. 318, 224-229.

LIU, A., FAN, J., FAN, M., 2015. *Quantum chemical calculations and molecular dynamics simulations of amine collector adsorption on quartz (0 0 1) surface in the aqueous solution*. Int. J. Miner. Process. 134, 1-10.

LIU, C.M., HU, Y.H., CAO, X.F., 2009. *Substituent effects in kaolinite flotation using dodecyl tertiary amines*. Miner. Eng. 22, 849-852.

LIU, G., XIAO, J., ZHOU, D., ZHONG, H., CHOI, P., XU, Z., 2013. *A DFT study on the structure-reactivity relationship of thiophosphorus acids as flotation collectors with sulfide minerals: Implication of surface adsorption*. Colloid. Surfaces. A. 434, 243-252.

LIU, W.G., ZHAO, L., LIU, W.B., YANG, T., DUAN, H., 2019. *Synthesis and utilization of a gemini surfactant as a collector for the flotation of hemimorphite from quartz*. Miner. Eng. 134, 394-401.

LIU, W.B., LIU, W.G., WEI, D.Z., LI, M.Y., ZHAO, Q., XU, S.C., 2017. *Synthesis of N,N-Bis(2-hydroxypropyl)laurylamine and its flotation on quartz*. Chem. Eng. J. 309, 63-69.

LIU, W.G., LIU, W.B., DAI, S.J., WANG, B.Y., 2018. *Adsorption of bis(2-hydroxy-3-chloropropyl) dodecylamine on quartz surface and its implication on flotation*. Results. Phys. 9, 1096-1101.

LIU, W.G., LIU, W.B., WANG, X.Y., WEI, D.Z., WANG, B.Y., 2016. *Utilization of novel surfactant N-dodecyl-isopropanolamine as collector for efficient separation of quartz from hematite*. Sep. Purif. Technol. 162, 188-194.

MANSOURI, K., RINGSTED, T., BALLABIO, D., TODESCHINI, R., CONSONNI, V., 2013. *Quantitative structure–*

activity relationship models for ready biodegradability of chemicals. J. Chem. Inf. Model. 53, 867-878.

NATARAJAN, R., NIRDOSH, I., 2003. *Application of topochemical, topostructural, physicochemical and geometrical parameters to model the flotation efficiencies of N-arylhydroxamic acids*. Int. J. Miner. Process. 71, 113-129.

NATARAJAN, R., NIRDOSH, I., 2006. *New collectors for sphalerite flotation*. Int. J. Miner. Process. 79, 141-148.

NATARAJAN, R., NIRDOSH, I., 2008. *Quantitative structure-activity relationship (QSAR) approach for the selection of chelating mineral collectors*. Miner. Eng. 21, 1038-1043.

NATARAJAN, R., NIRDOSH, I., 2009. *Effect of molecular structure on the kinetics of flotation of a Canadian nickel ore by N-arylhydroxamic acids*. Int. J. Miner. Process. 93, 284-288.

NATARAJAN, R., NIRDOSH, I., BASAK, S.C., MILLS, D.R., 2002. *QSAR modeling of flotation collectors using principal components extracted from topological indices*. J Chem Inf Comput Sci. 42, 1425-1430.

NOVICH, B., RING, T., 1985. *A predictive model for the alkylamine-quartz flotation system*. Langmuir. 1, 701-708.

RANDIC, M., 1975. *Characterization of molecular branching*. J. Am. Chem. Soc. 97, 6609-6615.

ROGERS, D., HOPFINGER, A.J., 1994. *Application of genetic function approximation to quantitative structure-activity relationships and quantitative structure-property relationships*. J. Chem. Inf. Comp. Sci. 34, 854-866.

SABLJIC, A., 2001. *QSAR models for estimating properties of persistent organic pollutants required in evaluation of their environmental fate and risk*. Chemosphere. 43, 363-375.

SAHOO, H., SINHA, N., RATH, S.S., DAS, B., 2015. *Ionic liquids as novel quartz collectors: Insights from experiments and theory*. Chem. Eng. J. 273, 46-54.

SHAHLAEI, M., 2013. *Descriptor Selection Methods in Quantitative Structure-Activity Relationship Studies: A Review Study*. Chem. Rev. 113, 8093-8103.

SHI, L.M., FAN, Y., MYERS, T.G., O'CONNOR, P.M., PAULL, K.D., FRIEND, S.H., WEINSTEIN, J.N., 1998. *Mining the NCI anticancer drug discovery databases: Genetic function approximation for the QSAR study of anticancer ellipticine analogues*. J. Chem. Inf. Comp. Sci. 38, 189-199.

SIVAKUMAR, P.M., BABU, S.K.G., MUKESH, D., 2007. *QSAR studies on chalcones and flavonoids as anti-tuberculosis agents using genetic function approximation (GFA) method*. Chem. Pharm. Bull. 55, 44-49.

SOMASUNDARAN, P., HEALY, T.W., FUERSTENAU, D., 1964. *Surfactant adsorption at the solid—liquid interface—dependence of mechanism on chain length*. J. Phys. Chem. 68, 3562-3566.

TODESCHINI, R., CONSONNI, V., 2008. *Handbook of molecular descriptors*. John Wiley & Sons.

VAZIRI HASSAS, B., KARAKAŞ, F., ÇELIK, M.S., 2014. *Ultrafine coal dewatering: Relationship between hydrophilic lipophilic balance (HLB) of surfactants and coal rank*. Int. J. Miner. Process. 133, 97-104.

WANG, D.Z., LIN, Q., JIANG, Y.R., 1996. *Molecular Design of Reagents for Mineral and Metallurgical Processing (in Chinese)*. Central south university of technology press.

WANG, X.Y., LIU, W.G., DUAN, H., LIU, W.B., 2018. *Degradation mechanism study of amine collectors in Fenton process by quantitative structure-activity relationship analysis*. Physicochem. Probl. Mi. 54, 713-721.

WILMSHURST, J., 1957. *Electronegativity of radicals. A method of calculation*. J. Chem. Phys. 27, 1129-1131.

WILMSHURST, J.K., 1959. *Empirical Expression for Ionic Character and the Determination of s Hybridization from Nuclear Quadrupole Coupling Constants*. J. Chem. Phys. 30, 561-565.

YANG, F., SUN, W., HU, Y.H., 2012. *QSAR analysis of selectivity in flotation of chalcopyrite from pyrite for xanthate derivatives: Xanthogen formates and thionocarbamates*. Miner. Eng. 39, 140-148.

YANG, X.L., ALBIJANIC, B., LIU, G.Y., ZHOU, Y., 2018a. *Structure-activity relationship of xanthates with different hydrophobic groups in the flotation of pyrite*. Miner. Eng. 125, 155-164.

YANG, X.L., ALBIJANIC, B., ZHOU, Y., ZHOU, Y., ZHU, X.N., 2018b. *Using 3D-QSAR to predict the separation efficiencies of flotation collectors: Implications for rational design of non-polar side chains*. Miner. Eng. 129, 112-119.

YU, X., ZHONG, H., LIU, G., 2008. *Current research status on cationic collector of reverse flotation desilication*. Light. Metals. 6, 6-10.

ZHANG, X.R., QIAN, Z.B., ZHENG, G.B., ZHU, Y.G., WU, W.G., 2017. *The design of a macromolecular depressant for galena based on DFT studies and its application*. Miner. Eng. 112, 50-56.

ZHU, Y., LUO, B., SUN, C., LIU, J., SUN, H., LI, Y., HAN, Y., 2016. *Density functional theory study of a-Bromolauric acid adsorption on the a-quartz (101) surface*. Miner. Eng. 92, 72-77.